

Crystalline-State Guest-Exchange and Gas-Adsorption Phenomenon for a “Soft” Supramolecular Porous Framework Stacking by a Rigid Linear Coordination Polymer

Sheng Hu, Kun-Huan He, Ming-Hua Zeng,* Hua-Hong Zou, and Yi-Min Jiang*

Key Laboratory of Medicinal Chemical Resources and Molecular Engineering, Department of Chemistry and Chemical Engineering, GuangXi Normal University, Guilin 541004, P.R. China

Received January 15, 2008

A 1D rigid, linear coordination polymer, (4,4'-bipyridine)(2-pyridylsulfonate)copper, has been applied for the controlled-assembly of a new porous host that generates 1D channels by an interdigitated packing through the recognition of hydrogen bonding and π - π stacking interactions. The porous structure is architecturally robust when it reversibly uptakes water molecules and exchanges guest small molecules (MeOH, *i*-PrOH) from solution as determined by single-crystal-to-single-crystal transformation studies. Moreover, the open-channel solid displays irreversible benzene and toluene vapor sorption behaviors attributed to a widening of the channel cross-section that fetters the larger guest molecules, resulting from the dynamic, “soft” supramolecular framework.

Introduction

The rapid development of microporous metal-organic frameworks (MOFs) has led to active discussion of their potential applications in gas storage,¹ separation,² ion-exchange,³ catalysis,⁴ and sensors.⁵ The design and control of porous-network structures is currently pressing demands for their applications. In recent years many porous MOFs with novel 0–3D porous structures that provide new sizes, shapes, and considerable internal surface environments have

been obtained,⁶ however, those low-dimensional systems with large, unoccupied lattice voids for entrapping and retaining specific guest molecules are rare.⁷ Furthermore, designing a porous structure with molecules that encode well-defined noncovalent motifs has recently become a new state-of-the-art. Among the noncovalent motifs, hydrogen bonding and π - π stacking have been employed as synthetic paradigms to rationally design superstructures.⁸ To answer the interesting question of how a porous framework can be constructed from a linear 1D polymer by design, a promising strategy is the rational choice of building-blocks with rigid molecular panels packed efficiently to create more opportunities for forming suitable lattice voids in a “soft” framework.^{7a}

On the other hand, a porous crystalline solid that has high capacity, good reversibility, fast reactivity, and sustainability

* To whom correspondence should be addressed. E-mail: zmh@mailbox.gxnu.edu.cn. Fax: 86 773 5846-279.

- (1) (a) Kubota, Y.; Takata, M.; Kobayashi, T. C.; Kitagawa, S. *Coord. Chem. Rev.* **2007**, *251*, 2510. (b) Eddaoudi, M.; Kim, J.; Rosi, N.; Vodak, D.; Wachter, J.; O'Keeffe, M.; Yaghi, O. M. *Science* **2002**, *295*, 469. (c) Rosi, N. L.; Eckert, J.; Eddaoudi, M.; Vodak, D. T.; Kim, J.; O'Keeffe, M.; Yaghi, O. M. *Science* **2003**, *300*, 1127.
- (2) (a) Bradshaw, D.; Prior, T. J.; Cussen, E. J.; Claridge, J. B.; Rosseinsky, M. J. *J. Am. Chem. Soc.* **2004**, *126*, 6106. (b) Uemura, K.; Kitagawa, S.; Kondo, M.; Fukui, K.; Kitaura, R.; Chang, H.-C.; Mizutani, T. *Chem.—Eur. J.* **2002**, *8*, 3586. (c) Min, K. S.; Suh, M. P. *Chem.—Eur. J.* **2001**, *7*, 303.
- (3) (a) Hoskins, B. F.; Robson, R. *J. Am. Chem. Soc.* **1990**, *112*, 1546. (b) Min, K. S.; Suh, M. P. *J. Am. Chem. Soc.* **2000**, *122*, 6834. (c) Yaghi, O. M.; Li, H. *J. Am. Chem. Soc.* **1996**, *118*, 295.
- (4) (a) Fujita, M.; Kwon, Y. J.; Washizu, S.; Ogura, K. *J. Am. Chem. Soc.* **1994**, *116*, 1151. (b) Seo, J. S.; Whang, D.; Lee, H.; Jun, S. I.; Oh, J.; Jeon, Y.; Kim, K. *Nature* **2000**, *404*, 982. (c) Wu, C.-D.; Hu, A.; Zhang, L.; Lin, W.-B. *J. Am. Chem. Soc.* **2005**, *127*, 8940.
- (5) (a) Albrecht, M.; Lutz, M.; Spek, A. L.; Van Koten, G. *Nature* **2000**, *406*, 970. (b) Real, J. A.; Andrés, E.; Muñoz, M. C.; Julve, M.; Granier, T.; Bousseksou, A.; Varret, F. *Science* **1995**, *268*, 265. (c) Beauvais, L. G.; Shores, M. P.; Long, J. R. *J. Am. Chem. Soc.* **2000**, *122*, 2763.

- (6) (a) James, S. L. *Chem. Soc. Rev.* **2003**, *32*, 276; and references therein. (b) Bradshaw, D.; Claridge, J. B.; Cussen, E. J.; Prior, T. J.; Rosseinsky, M. J. *Acc. Chem. Res.* **2005**, *38*, 273. (c) Kitagawa, S.; Matsuda, R. *Coord. Chem. Rev.* **2007**, *251*, 2490. (d) Lin, X.; Jia, J.-H.; Hubberstey, P.; Schröder, M.; Champness, N. R. *CrystEngComm* **2007**, *9*, 438.
- (7) (a) Takamizawa, S.; Nakata, E.; Yokoyama, H.; Mochizuki, K.; Mori, W. *Angew. Chem., Int. Ed.* **2003**, *42*, 4331. (b) Bobrzańska, L.; Lloyd, G. O.; Raubenheimer, H. G.; Barbour, L. J. *J. Am. Chem. Soc.* **2005**, *127*, 13134. (c) Mahmoudkhani, A. H.; Shimizu, G. K. H. *Inorg. Chem.* **2007**, *46*, 1593. (d) Lee, E. Y.; Suh, M. P. *J. Am. Chem. Soc.* **2004**, *43*, 2798. (e) Cingolani, A.; Galli, S.; Masciocchi, N.; Pandolfo, L.; Pettinari, C.; Sironi, A. *J. Am. Chem. Soc.* **2005**, *127*, 6144.
- (8) (a) Malek, N.; Maris, T.; Simard, M.; Wuest, J. D. *J. Am. Chem. Soc.* **2005**, *127*, 5910. (b) Uemura, K.; Saito, K.; Kitagawa, S.; Kita, H. *J. Am. Chem. Soc.* **2006**, *128*, 16122.

may be suitable for the potential applications in guest-exchange, gas-adsorption, crystalline reaction, and separation of specific molecules, as evidenced in our and previous groups' papers.^{9,10} Following the above consideration, we report herein a novel porous material constructed by a rigid, linear 1D coordination polymer, namely [Cu(2-pySO₃)₂(bpy)]·H₂O (**1**·H₂O) (2-pySO₃ = 2-pyridine-sulfonate, bpy = 4,4'-bipyridine), which is structurally characterized by single-crystal X-ray diffraction in both solvated and desolvated forms. As will be shown, a discrete linear 1D coordination polymer is effectively controlled by the ideal linkers bpy ligands when 2-pySO₃ ligands chelate octahedral Cu(II) forming a molecular panel. The panels of the staggeredly stacked 1D chain create interlinked lattice voids, which can be used for crystal-to-crystal guest exchange and exhibit unique sorption behaviors.

Experimental Section

Materials and Physical Measurements. The reagents and solvents employed were commercially available and used as received without further purification. The C, H, and N microanalyses were carried out with an Elementar Vario-EL CHNS elemental analyzer. The FT-IR spectra were recorded from KBr pellets in the range 4000–400 cm⁻¹ on a Bio-Rad FTS-7 spectrometer. X-ray powder diffraction (XRPD) intensities were measured at 293 K on a Rigaku D/max-III A diffractometer (Cu-Kα, λ = 1.54056 Å). The single-crystalline powder samples were prepared by crushing the crystals and scanned from 3–60° with a step of 0.1°/s. Calculated patterns of **1**·H₂O were generated with PowderCell. The sorption isotherms for methanol and benzene vapors were measured with an automatic gravimetric adsorption apparatus (IGA-003 series, Hiden Isochema Ltd.) at 298 K. The as-synthesized samples (weight 250–300 mg) were placed in a quartz tube and dried under high vacuum at 393 K for 12 h to remove the solvent molecules prior to measurements.

Hydrothermal Syntheses. A mixture of Cu(NO₃)₂·3H₂O (0.241 g, 1.0 mmol), NaOH (0.080 g, 2.0 mmol), pyridine-2-sulfonic acid (0.316 g, 2.0 mmol), and H₂O (8.0 mL) was stirred for 10 min in air. 4,4'-Bipyridine (0.156 g, 1.0 mmol) in MeOH (8 mL) was then added, and the reaction continued for another 10 min. Then, the mixture was placed in a 23-mL Teflon-lined autoclave and heated at 130 °C for 72 h. The autoclave was cooled over a period of 16 h at a rate of 5 °C h⁻¹, and **1**·H₂O as blue block crystals were collected by filtration, washed with water, and dried at ambient temperature. Yield: 50.8% (based on Cu). Element analyses for **1**·H₂O: C₂₀H₁₈CuN₄O₇S₂ (554.04); Calcd (%): C, 43.36; H, 3.27;

N, 10.11. Found (%): C, 42.82; H, 3.40; N, 9.77. IR for **1**·H₂O (KBr, cm⁻¹): 3449s, 3100w, 2927w, 1611m, 1536w, 1493w, 1419m, 1218s, 1099s, 1072s, 1028s, 813w, 828w, 739w, 631m.

Preparations of **1·MeOH and **1**·*i*-PrOH.** After immersing proper sized crystals of **1**·H₂O in MeOH or *i*-PrOH solvents in small sealed tubes, respectively, at room temperature for 1 day, the crystals retained their well-defined external forms with the microporous space accommodating new guest molecules, furnishing crystals of **1**·MeOH and **1**·*i*-PrOH, respectively, which are stable in the atmosphere. The IR spectrum of **1**·MeOH shows absorptions at 3465m, 2967w, 2926w, 1072s, and 1057m cm⁻¹, which can be attributed to the characteristic vibrations of MeOH, while that of **1**·*i*-PrOH shows absorptions at 3487m, 2963w, 2924w, 2905w, 1384w, 1299m, 1169m, 1153s, 1099m, 1057s, and 865w cm⁻¹, which can be attributed to the characteristic vibrations of *i*-PrOH.

Rehydration of **1.** Standing the tested single crystal sample of **1** in air (*T* = 22(2) °C, relative humidity = 35(5) %) for 24 h gave rise to the rehydrated **1**'.

X-ray Crystallography. Diffraction intensities of **1**·H₂O, **1**, **1**', **1**·MeOH, and **1**·*i*-PrOH were collected on a Bruker Apex CCD area-detector diffractometer (Mo-Kα, λ = 0.71073 Å). Absorption corrections were applied by using the multiscan program SADABS.¹¹ The structures were solved with direct methods and refined with a full-matrix least-squares technique with the SHELXTL program package.¹² Anisotropic thermal parameters were applied to all nonhydrogen atoms. The organic hydrogen atoms were generated geometrically (C–H 0.96 Å); the aqua hydrogen atoms were located from difference maps and refined with isotropic temperature factors. The disorder was treated by performing half-occupancies with C and O atoms of the guest molecules. Crystal data, as well as details of data collection and refinements for complexes **1**·H₂O, **1**, **1**', **1**·MeOH, and **1**·*i*-PrOH, are summarized in Table 1. Selected bond distances and bond angles are listed in Table 2.

Results and Discussion

Crystal Structures. Single-crystal X-ray crystallographic studies revealed that complex **1**·H₂O exhibits an infinite, rigid, linear polymeric chain consisting of [Cu(2-pySO₃)₂]₂ square building fragments connected by bpy linkers. In the crystallographically asymmetric unit there is one octahedral Cu^{II} atom, lying on a special position, one 2-pySO₃ chelating ligand, one-half of bpy, and one guest water molecule with one-half occupancy. The local coordination geometry of Cu^{II} in **1**·H₂O is shown in Figure 1. Two 2-pySO₃ ligands adopt chelating mode using their sulfonate groups and pyridine groups and create four-coordination at the equatorial plane of the octahedral Cu^{II} atom, forming a square building fragment (Cu–O 2.298(3) Å, Cu–N 2.025(3) Å). The axial sites of Cu^{II} atom are occupied by two N atoms of bpy ligands, which bridge the [Cu(2-pySO₃)₂] fragments to a perfectly linear chain (N(2)–Cu(1)–N(3b) 180°). The bpy ligand is twisted with a dihedral angle of 32.45(2)° between the pair of pyridyl rings. Interestingly, these linear chains run parallel to the *b* axis and no interweavement of chains occurs.^{9d}

- (9) (a) Zeng, M.-H.; Feng, X.-L.; Chen, X.-M. *Dalton Trans.* **2004**, 2217. (b) Zeng, M.-H.; Feng, X.-L.; Zhang, W.-X.; Chen, X.-M. *Dalton Trans.* **2006**, 5294. (c) Hu, S.; Zhang, J.-P.; Li, H.-X.; Tong, M.-L.; Chen, X.-M.; Kitagawa, S. *Cryst. Growth Des.* **2007**, 7, 2286. (d) Zeng, M.-H.; Zhang, W.-X.; Sun, X.-Z.; Chen, X.-M. *Angew. Chem., Int. Ed.* **2005**, 44, 3079. (e) Zeng, M.-H.; Gao, S.; Yu, X.-L.; Chen, X.-M. *New J. Chem.* **2003**, 27, 1599.
- (10) (a) Zhang, J. P.; Kitagawa, S. *J. Am. Chem. Soc.* **2008**, 130, 907. (b) Pan, L.; Parker, B.; Wang, X.; Olson, D. H.; Lee, J.; Li, J. *J. Am. Chem. Soc.* **2006**, 128, 4180. (c) Pan, L.; Olson, D. H.; Ciemmolonski, L. R.; Heddy, R.; Huang, X.-Y.; Li, J. *Angew. Chem., Int. Ed.* **2006**, 45, 616. (d) Walton, K. S.; Millward, A. R.; Dubbeldam, D.; Frost, H.; Low, J. J.; Yaghi, O. M.; Snurr, R. Q. *J. Am. Chem. Soc.* **2008**, 130, 406. (e) Ma, S.-Q.; Sun, D.-F.; Simmons, J. M.; Collier, C.-D.; Yuan, D.-Q.; Zhou, H.-C. *J. Am. Chem. Soc.* **2008**, 130, 1012. (f) Haneda, T.; Kawano, M.; Kawamichi, T.; Fujita, M. *J. Am. Chem. Soc.* **2008**, 130, 1578.

(11) Sheldrick, G. M. *SADABS* Version 2.05; University Göttingen: Göttingen, Germany.

(12) *SHELXTL 6.10*; Bruker Analytical Instrumentation: Madison, WI, 2000.

Table 1. Crystal Data and Structure Refinements for **1**·H₂O, **1**, **1'**, **1**·MeOH, and **1**·*i*-PrOH

	1 ·H ₂ O	1	1'	1 ·MeOH	1 · <i>i</i> -PrOH
formula	C ₂₀ H ₁₈ CuN ₄ O ₇ S ₂	C ₂₀ H ₁₆ CuN ₄ O ₆ S ₂	C ₂₀ H ₁₈ CuN ₄ O ₇ S ₂	C ₂₁ H ₂₀ CuN ₄ O ₇ S ₂	C ₂₁ H ₂₄ CuN ₄ O ₇ S ₂
formula weight	554.04	536.02	554.04	568.08	596.12
temp/K	293(2)	393(2)	173(2)	293(2)	173(2)
cryst syst	monoclinic	monoclinic	monoclinic	monoclinic	monoclinic
space group	<i>P2/c</i>	<i>P2/c</i>	<i>P2/c</i>	<i>P2/c</i>	<i>P2/c</i>
<i>a</i> /Å	10.839(8)	10.873(3)	10.767(3)	10.748(5)	10.840(5)
<i>b</i> /Å	11.142(8)	11.153(3)	11.145(3)	11.127(6)	11.144(5)
<i>c</i> /Å	10.899(8)	10.897(3)	10.847(3)	10.840(6)	10.864(5)
β /deg	102.925(8)	102.871(4)	103.011(5)	102.400(9)	102.604(8)
<i>V</i> /Å ³	1283.0(2)	1288.1(5)	1268.3(6)	1266.0(1)	1280.0(1)
<i>Z</i>	2	2	2	2	2
<i>D_c</i> /g cm ⁻³	1.434	1.382	1.451	1.490	1.546
μ /mm ⁻¹	1.059	1.049	1.071	1.075	1.066
<i>F</i> (000)	566	546	566	582	614
no. of rflns collected	11320	6977	6650	6194	8185
no. of indep rflns	3179	2768	2777	2718	2780
<i>R</i> _{int}	0.0344	0.0300	0.0398	0.0502	0.0396
GO _F	1.139	1.086	1.090	1.076	1.067
<i>R</i> 1 ^a (<i>I</i> > 2σ(<i>I</i>))	0.0736	0.0473	0.0509	0.0534	0.0420
w <i>R</i> 2 ^a (all data)	0.2240	0.1506	0.1504	0.1516	0.1090

$$^a R_1 = \sum(|F_o| - |F_c|)/\sum|F_o|, wR_2 = [\sum w(F_o^2 - F_c^2)^2/\sum w(F_o^2)^2]^{1/2}.$$

Each chain slips and obstructs the neighboring chains with flanking arms, forming an interdigitated packing motif. As shown in Figure 2, the pyridyl rings of 2-pySO₃ of neighboring chains stack with each other, and the face-to-face and centroid-centroid distances are about 3.42 and 3.86 Å, respectively, indicating significant π - π interaction. A C-H $\cdots\pi$ interaction with an H(3) \cdots centroid distance of 3.73 Å is also found to interlink the adjacent chains between the flanking pyridyl ring of 2-pySO₃ and the pyridyl ring of bpy. The π - π stacking interaction is an important supramolecular force to govern the process of recognition and self-assembly¹³ of the linear chains in a parallel fashion, resulting in the formation of a complementary aromatic stacking 2D grid which lies in the (101) crystallographic plane and contains openings of a minimum size 4.96 × 4.89 Å excluding van der Waals radii.

These layers are further stacked into a 3D supramolecular MOF with 1D channels (Figure 3), where the interlayer C-H \cdots O contacts between neighboring aromatic C-H groups of bpy and the oxygen atoms of sulfonate groups of 2-pySO₃ are found,¹⁴ and the C \cdots O distances and the C-H \cdots O angles are in the ranges 3.27–3.37 Å and 123.4–139.9 Å, respectively. The 1D channels are enclosed by the aromatic rings of bpy and 2-pySO₃ while the space between the adjacent 2D grids is less than 0.7 Å assuming van der Waals radii. Therefore, only the translational motion of the guest molecules along the (101) direction is permissible, shown in Figure 4.

The diagonal lengths and effective window size of the channels are about 3.79 × 3.79 Å and 5.27 × 4.92 Å (taking account of the van der Waals radii) calculated by the spaces between the oxygen atoms of sulfonate groups, the aromatic C-H groups of bpy and 2-pySO₃, respectively. The solvent accessible volume *V*_{void} of **1** is 23.9% as calculated by PLATON.¹⁵ The water guest molecules are located in the

channels and in close contact with the sulfonate groups of the adjacent polymeric chains [C \cdots O = 2.980(1) Å; C-H \cdots O = 153.7°]. To the best of our knowledge, only few of the crystal structures of metal-organic complexes with 2-pySO₃ ligand have been documented.¹⁶ 4,4'-Bipyridine has been employed as an effective linker between the transition metal atoms for the propagation of the coordination network. Of the polymers of bpy with transition metals, there are many possible structures: linear chains, zigzag chains, double, triple, and quadruple chains, ladders, molecular antennas, railroads, 4-fold helices, bilayers, square grids, rectangular grids, Lincoln Log, 3D frameworks, and 4²·8² topology diamondoid and cubic geometries, but most of them are linear chains.¹⁷ In the present case, a molecular panel with the bis-(2-pySO₃) chelated Cu(II) atom is critical in the formation of the chain structure.

Thermal Stability. The thermogravimetric analysis (TGA) was carried out to examine the thermal stability and capacity of **1**·H₂O. On heating **1**·H₂O to 900 °C in N₂, three weight loss steps were observed in the TG curve that were accompanied with endothermic events in the differential thermal analysis (DTA) curve (Figure 5). The TGA curve for **1**·H₂O showed that the first weight loss of 3.4% between 20 and 87 °C corresponds to the loss the first weight loss of guest water molecules (calcd 3.3%) in the channels. The anhydrous host MOF, or **1**, remained stable up to ~170 °C. The decomposition of **1** began at 170 °C; in the temperature range 170–232 °C, the pyrolysis of bpy occurred with a loss of 28.7% (calcd 28.1%). Therefore, it can be assumed that during this thermal reaction [Cu(2-pySO₃)₂] fragments are formed, which decomposed in the temperature range

(13) Moulton, B.; Zaworotko, M. J. *Chem. Rev.* **2001**, *101*, 1629.(14) May, L. J.; Shimizu, G. K. H. *Chem. Commun.* **2005**, 1270.(15) Spek, A. L. *PLATON, A Multipurpose Crystallographic Tool*; Utrecht University: Utrecht, The Netherlands, 2000.(16) (a) Charbonnier, F.; Faure, R.; Loiseau, H. *Cryst. Struct. Commun.* **1981**, *10*, 1129. (b) Delgado, S.; Molina-Ontoria, A.; Medina, M. E.; Pastor, C. J.; Jimenez-Aparicio, R.; Priego, J. L. *Inorg. Chem. Commun.* **2006**, *9*, 1289. (c) Lobana, T. S.; Kinoshita, I.; Kimura, K.; Nishioka, T.; Shiomi, D.; Isobe, K. *Eur. J. Inorg. Chem.* **2004**, 356.(17) (a) Biradha, K.; Sarkar, M.; Rajput, L. *Chem. Commun.* **2006**, 4169. (b) Chen, X.-M.; Tong, M.-L. In *Frontiers in Crystal Engineering*; Tiekink, E., Vittal, J. J., Eds.; John-Wiley & Son Ltd: New York, 2006; Chapter 10, pp 219–259. (c) Janiak, C. J. *Chem. Soc., Dalton Trans.* **2003**, 2781; and references therein.

Table 2. Bond Lengths (Å) and Angles (°) for **1**·H₂O, **1**, **1'**, **1**·MeOH, and **1**·*i*-PrOH^a

1 ·H ₂ O			
Cu(1)–N(1a)	2.023(5)	Cu(1)–N(3b)	2.047(6)
Cu(1)–N(1)	2.023(5)	Cu(1)–O(1)	2.304(4)
Cu(1)–N(2)	2.041(6)	Cu(1)–O(1a)	2.304(4)
N(1)–Cu(1)–N(1a)	179.7(3)	N(2)–Cu(1)–O(1)	93.5(1)
N(1)–Cu(1)–N(2)	89.9(1)	N(3b)–Cu(1)–O(1)	86.5(1)
N(1a)–Cu(1)–N(2)	89.9(1)	N(1)–Cu(1)–O(1a)	99.3(2)
N(1)–Cu(1)–N(3b)	90.1(1)	N(1a)–Cu(1)–O(1a)	80.7(2)
N(1a)–Cu(1)–N(3b)	90.1(1)	N(2)–Cu(1)–O(1a)	93.5(1)
N(2)–Cu(1)–N(3b)	180.0	N(3b)–Cu(1)–O(1a)	86.5(1)
N(1)–Cu(1)–O(1)	80.7(2)	O(1)–Cu(1)–O(1a)	172.9(2)
N(1a)–Cu(1)–O(1)	99.3(2)		
1			
Cu(1)–N(1)	2.025(3)	Cu(1)–N(3b)	2.064(4)
Cu(1)–N(1a)	2.025(3)	Cu(1)–O(1)	2.298(3)
Cu(1)–N(2)	2.041(4)	Cu(1)–O(1a)	2.298(3)
N(1)–Cu(1)–N(1a)	180.0	N(2)–Cu(1)–O(1)	93.7(6)
N(1)–Cu(1)–N(2)	89.9(7)	N(3b)–Cu(1)–O(1)	86.4(6)
N(1a)–Cu(1)–N(2)	89.9(7)	N(1)–Cu(1)–O(1a)	98.0(1)
N(1)–Cu(1)–N(3b)	90.0(7)	N(1a)–Cu(1)–O(1a)	81.0(1)
N(1a)–Cu(1)–N(3b)	90.0(7)	N(2)–Cu(1)–O(1a)	93.7(6)
N(2)–Cu(1)–N(3b)	180.0	N(3b)–Cu(1)–O(1a)	86.4(6)
N(1)–Cu(1)–O(1)	81.0(1)	O(1)–Cu(1)–O(1a)	172.7(1)
N(1a)–Cu(1)–O(1)	98.0(1)		
1'			
Cu(1)–N(1)	2.024(3)	Cu(1)–N(3b)	2.051(4)
Cu(1)–N(1a)	2.024(3)	Cu(1)–O(1a)	2.296(3)
Cu(1)–N(2)	2.041(4)	Cu(1)–O(1)	2.296(3)
N(1)–Cu(1)–N(1a)	179.1(2)	N(2)–Cu(1)–O(1a)	93.4(6)
N(1)–Cu(1)–N(2)	89.6(9)	N(3b)–Cu(1)–O(1a)	86.6(7)
N(1a)–Cu(1)–N(2)	89.6(9)	N(1)–Cu(1)–O(1)	81.5(1)
N(1)–Cu(1)–N(3b)	90.4(9)	N(1a)–Cu(1)–O(1)	98.6(1)
N(1a)–Cu(1)–N(3b)	90.4(9)	N(2)–Cu(1)–O(1)	93.4(7)
N(2)–Cu(1)–N(3b)	180.0	N(3b)–Cu(1)–O(1)	86.6(6)
N(1)–Cu(1)–O(1a)	98.6(1)	O(1a)–Cu(1)–O(1)	173.1(2)
N(1a)–Cu(1)–O(1a)	81.5(1)		
1 ·MeOH			
Cu(1)–N(1a)	2.027(3)	Cu(1)–N(3b)	2.055(4)
Cu(1)–N(1)	2.027(3)	Cu(1)–O(1a)	2.299(3)
Cu(1)–N(2)	2.035(4)	Cu(1)–O(1)	2.299(3)
N(1a)–Cu(1)–N(1)	179.3(2)	N(2)–Cu(1)–O(1a)	93.6(7)
N(1a)–Cu(1)–N(2)	89.6(9)	N(3b)–Cu(1)–O(1a)	86.4(7)
N(1)–Cu(1)–N(2)	89.6(9)	N(1a)–Cu(1)–O(1)	98.7(1)
N(1a)–Cu(1)–N(3b)	90.4(9)	N(1)–Cu(1)–O(1)	81.4(1)
N(1)–Cu(1)–N(3b)	90.4(9)	N(2)–Cu(1)–O(1)	93.6(7)
N(2)–Cu(1)–N(3b)	180.0	N(3b)–Cu(1)–O(1)	86.4(7)
N(1a)–Cu(1)–O(1a)	81.4(1)	O(1a)–Cu(1)–O(1)	172.8(1)
N(1)–Cu(1)–O(1a)	98.7(1)		
1 · <i>i</i> -PrOH			
Cu(1)–N(1a)	2.021(2)	Cu(1)–N(3b)	2.053(3)
Cu(1)–N(1)	2.021(2)	Cu(1)–O(1)	2.298(2)
Cu(1)–N(2)	2.040(3)	Cu(1)–O(1a)	2.298(2)
N(1a)–Cu(1)–N(1)	179.4(1)	N(2)–Cu(1)–O(1)	93.5(5)
N(1a)–Cu(1)–N(2)	89.7(6)	N(3b)–Cu(1)–O(1)	86.5(5)
N(1)–Cu(1)–N(2)	89.7(6)	N(1a)–Cu(1)–O(1a)	81.5(9)
N(1a)–Cu(1)–N(3b)	90.3(6)	N(1)–Cu(1)–O(1a)	98.5(9)
N(1)–Cu(1)–N(3b)	90.3(6)	N(2)–Cu(1)–O(1a)	93.5(5)
N(2)–Cu(1)–N(3b)	180.0	N(3b)–Cu(1)–O(1a)	86.5(5)
N(1a)–Cu(1)–O(1)	98.5(9)	O(1)–Cu(1)–O(1a)	173.0(10)
N(1)–Cu(1)–O(1)	81.5(9)		

^a Symmetry codes: (a) $-x + 1/2, y, -z + 1/2$; (b) $x, y - 1, z$.

232–900 °C. The resulting amorphous phase crystallizes at higher temperature to give CuO.¹⁸

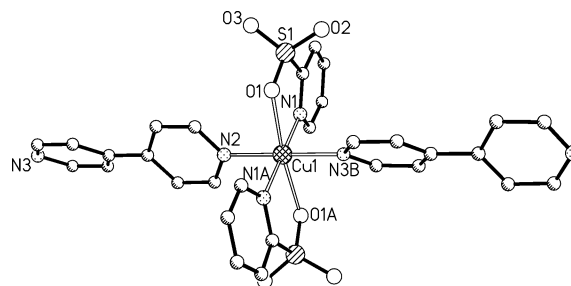


Figure 1. Coordination environment in **1**·H₂O (some equivalent atoms have been generated to complete the Cu coordination, H atom omitted for clarity).

Single-Crystal-to-Single-Crystal Guest Exchange. The channels can reversibly take up water and exchange guest molecules from solution, such as methanol, isopropanol, and the new phases of **1**, **1'**, **1**·MeOH, and **1**·*i*-PrOH have been fully characterized by single-crystal X-ray diffraction (Figure 6), providing insight into the ability of the host lattice in accommodating the guests.^{9,19} We directly observed by crystallography the *in situ* reversible uptake of water. The single-crystal diffraction data of dehydrated **1** were measured by using the as-synthesized crystal **1**·H₂O heated at 100 °C under N₂ atmosphere, and the result confirms that no significant change of the framework structure occurs after dehydration while the space previously occupied by water molecules becomes devoid of any appreciable electron density. More interestingly, the dehydration process can be reversed by exposing this dehydrated crystal sample to the atmosphere for 24 h, giving the rehydrated phase **1'**, which could be directly used for single-crystal diffraction. Moreover, when the single crystals of **1**·H₂O were soaked for 1 day in two different solvents, methanol and isopropanol, at room temperature, they turned into **1**·MeOH and **1**·*i*-PrOH, respectively. During the transformation of **1**·H₂O into **1**·MeOH and **1**·*i*-PrOH, both **1**·MeOH and **1**·*i*-PrOH are isomorphous to **1**·H₂O and contain one guest molecule per formula unit, which is located in the channel. No substantial change was observed in the unit-cell parameters and the window size of the 1D channels in comparison to the parent host lattice. Figure 7 shows the main host–guest interactions. Methanol dimers were observed in the channel of **1**·MeOH. Only weak C–H···O hydrogen-bonding interactions are present between the methyl hydrogen atoms of MeOH and the noncoordinated oxygen atoms of sulfonate groups of the host framework (C···O, 3.25 Å). In **1**·*i*-PrOH, the sulfonate groups also provide hydrogen bonding sites and are associated with oxygen atoms of *i*-PrOH at a distance of 2.94 Å. The observation of the guest-exchange phenomenon further confirms the insolubility and stability of the porous framework constructed by 1D linear polymer chains.¹⁹ TG analyses of crystalline samples of the guest-exchanged with MeOH, *i*-PrOH, benzene, and toluene showed the release of guest molecules in different steps (Supporting Information, Figure S1). The guest molecules, the weight loss observed (%), and

(18) Lin, X.; Jia, J.-H.; Zhao, X.-B.; Thomas, K. M.; Blake, A. J.; Walker, G. S.; Champness, N. R.; Hubberstey, P.; Schröder, M. *Angew. Chem., Int. Ed.* **2006**, *45*, 7358.

(19) Kawano, M.; Fujita, M. *Coord. Chem. Rev.* **2007**, *251*, 2592.

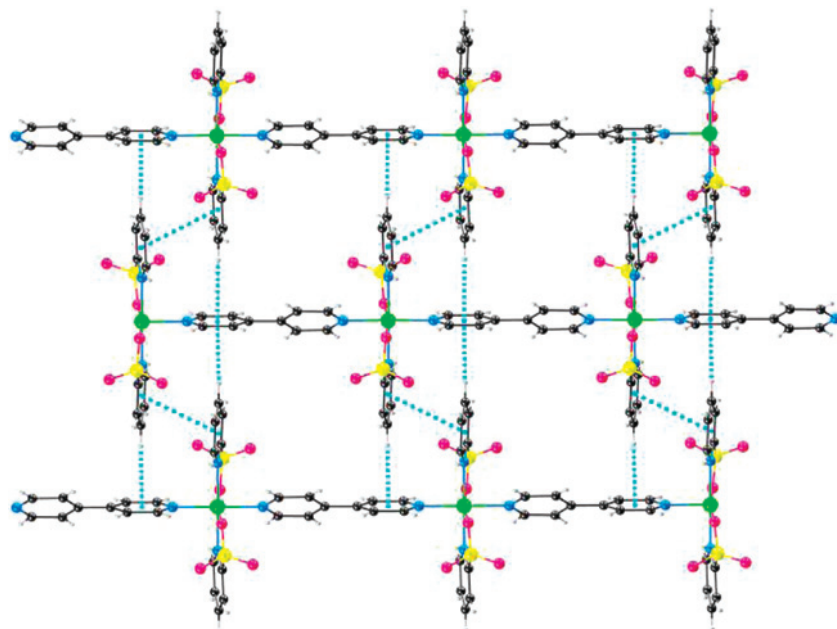


Figure 2. Complementary aromatic stacking layer formed by linear chains in $1 \cdot \text{H}_2\text{O}$. Colors: carbon, gray; hydrogen, white; nitrogen, sky blue; oxygen, red; sulfur, yellow; copper, green. Hereafter, the plots use the same color scheme.

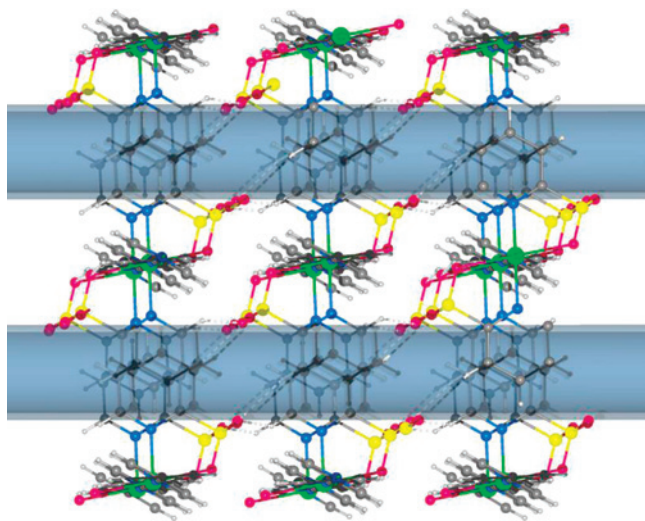


Figure 3. (a) View of $1 \cdot \text{H}_2\text{O}$ on the ac plane showing the weak hydrogen-bonding interaction between aromatic stacking 2D layers (guests H_2O are omitted for clarity, 1D channels are highlighted as powder blue columns).

the temperature ($^{\circ}\text{C}$) are as follows: MeOH, 5.5, about 125; *i*-PrOH, 8.3, about 156. This is in agreement with the crystallographic analyses.

Gas Sorption Properties. The porosity of **1** was further verified by vapor adsorption. The sorption isotherm of methanol vapor was measured at 40°C . As shown in Figure 8, the sorption of **1** for methanol shows gradual increases in the pressure range ($P/P_0 = 0.01$ – 0.89) without saturation, and the amount adsorbed is $99.8 \text{ mg} \cdot \text{g}^{-1}$ (1.6 MeOH molecules per formula unit) at $P/P_0 = 0.89$, which indicates the diffusion of MeOH guest molecules (size $3.8 \times 3.9 \text{ \AA}$) into the channels. The adsorption and desorption experiments with MeOH trace the same isotherms, which indicates that the channel structure is retained through this process.²⁰

To test the flexibility of **1**, we carried out adsorption/desorption experiments by using two large guest molecules,

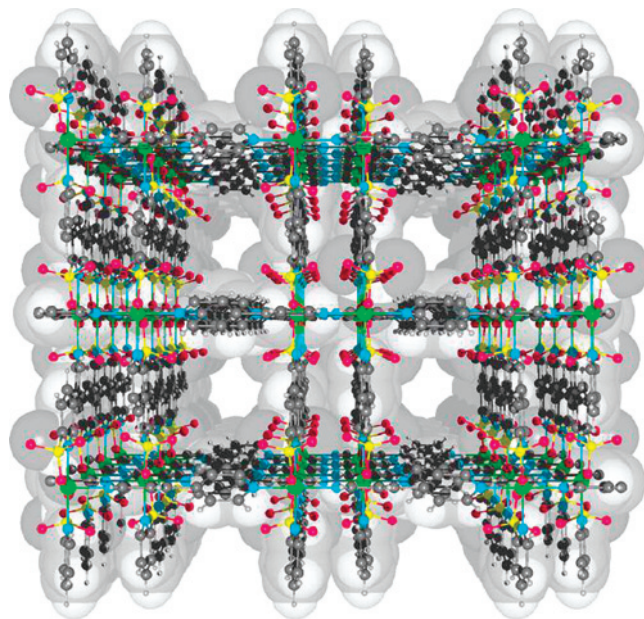


Figure 4. Ball-and-stick and space-filling diagram direction showing the packing arrangement of host complexes along (101).

benzene (size $3.3 \times 6.6 \text{ \AA}$) and toluene (size $4.0 \times 6.6 \text{ \AA}$). The sorption isotherms of benzene and toluene vapor were measured at 40°C . The sorption of **1** for benzene and toluene shows gradual increases in the pressure range (0.01 – 0.77 and 0.01 – 0.89) without saturation, and that approximately 1/2 and 1/8 of benzene and toluene molecules, respectively, were adsorbed per formula unit of **1**. The desorption curves of benzene and toluene do not coincide with the adsorption curves, showing no significant desorption, which suggest that benzene and toluene molecules fettered in the cavities.²¹ In consideration of the size difference between the pore aperture ($5.27 \times 4.92 \text{ \AA}$) and the guest molecules, as well as that the wall of the cavity is suitable to render π - π or $\text{C}-\text{H} \cdots \pi$ interactions between the phenyl guests and the aromatic rings

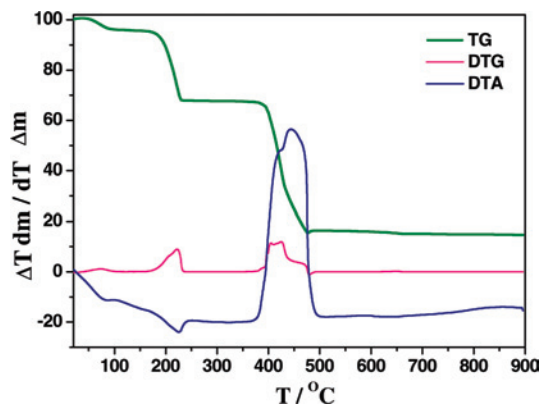


Figure 5. TG, DTG, and DTA curves for an as-synthesized sample of $1 \cdot \text{H}_2\text{O}$ under a dinitrogen atmosphere.

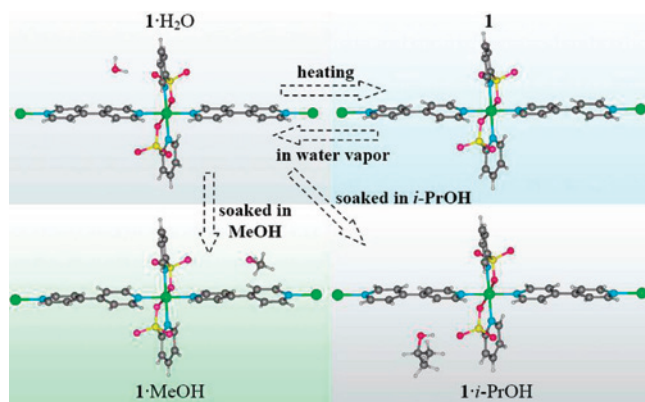


Figure 6. Summary of the crystalline-state guest exchange.

of 2-pySO₃ and bpy in **1**, there should be a slight distortion of the host framework when large guest molecules diffuse into the small cavities. As shown in the structural detail of **1**, the parallel 1D linear chains loosely stack for the possible sliding movement whereas the pyridyl groups of bpy can rotate along the central C–C bond, which implies that the large guest incorporated inside the crystal can diffuse through the expandable windows of the channels and fettered in the cavities. Therefore, the weak interactions consolidated supramolecular framework of the 1D chains can expand cavities to accommodate larger molecules.²² The above observations indicate that, as a small molecule, MeOH has only weak C–H···O interactions with the host framework, and thus has the highest reversible sorption among these three kinds of species. In contrast, the rigid and oversize benzene or toluene not only leads to less uptakes but also exhibit basically irreversible sorption, owing to distortion of the host framework and the stronger π – π interactions with the host framework. Thus, the different types of isotherms of guest molecules in a porous framework can depend on the cooperative effect of several factors, such as supramolecular

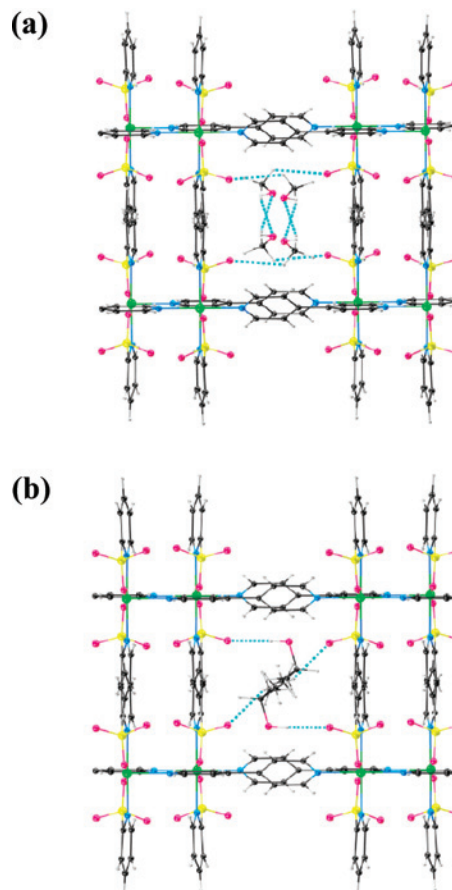


Figure 7. View of the narrowest part of the 1D channels in (a) $1 \cdot \text{MeOH}$ and (b) $1 \cdot i\text{-PrOH}$ showing the host–guest interactions.

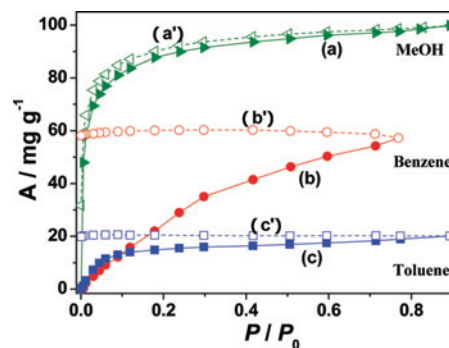


Figure 8. Adsorption isotherms for different adsorbates in **1** at 313 K, (a) MeOH; (b) benzene, and (c) toluene, and desorption isotherms for different adsorbates in **1** at 313K, (a') MeOH, (b') benzene, and (c') toluene.

interactions and the size of the guest.²⁰ The isotherms were difficult to be fitted by using the Dubinin–Radushkevich (DR) equation to characterize the “dynamic” porosity of **1**.^{1a}

Solid-State-Liquid Guest Inclusion. To further check the oversized guest molecules inclusion properties of **1** and to examine if the framework can reversibly expand the window size upon the above process, a crystalline sample of $1 \cdot \text{H}_2\text{O}$ was dried under vacuum at 120 °C for 0.5 h and then immersed in benzene and toluene. Comparison of XRPD patterns between **1**, $1 \cdot \text{H}_2\text{O}$, and the immersed products shows that a few new peaks appeared and some peaks disappeared between 7–20°, although most other diffraction peaks could be observed in comparison to that of $1 \cdot \text{H}_2\text{O}$ (Figure 9). These observations suggest that the adsorption of oversize guests

- (20) (a) Noro, S.; Kitagawa, S.; Kondo, M.; Seki, K. *Angew. Chem., Int. Ed.* **2000**, *39*, 2082. (b) Bu, X.-H.; Tong, M.-L.; Chang, H.-C.; Kitagawa, S.; Batten, S. R. *Angew. Chem., Int. Ed.* **2004**, *43*, 192. (c) Lin, X.; Blake, A. J.; Wilson, C.; Sun, X.-Z.; Champness, N. R.; George, M. W.; Hubberstey, P.; Mokaya, R.; Schröder, M. *J. Am. Chem. Soc.* **2006**, *128*, 10745.
- (21) Xue, D.-X.; Lin, Y.-Y.; Cheng, X.-N.; Chen, X.-M. *Cryst. Growth Des.* **2007**, *7*, 1332.
- (22) Maji, T. K.; Uemura, K.; Chang, H.-C.; Matsuda, R.; Kitagawa, S. *Angew. Chem., Int. Ed.* **2004**, *46*, 889.

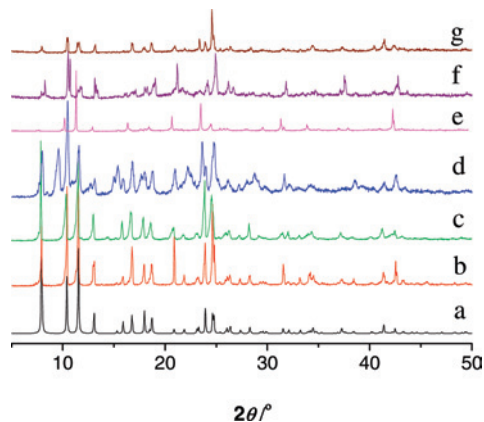


Figure 9. XRPD patterns of (a) simulated $1 \cdot \text{H}_2\text{O}$, (b) as-synthesized $1 \cdot \text{H}_2\text{O}$, (c) guest-free of **1**, dried crystals **1** immersed in benzene (d), toluene (e), *o*-methoxyphenol (f), and 1-chloronaphthalene (g).

is followed by a slight structural change of the “soft” supramolecular framework. TG analyses indicate that the mass steps of $1 \cdot x(\text{benzene})$ and $1 \cdot y(\text{toluene})$ are not well-resolved, and therefore, the mass loss is difficult to estimate, consistent with the sorption behaviors. However, the experimental mass loss of the steps of about 7.7% (benzene) and 1.7% (toluene) are in the reasonable range in reference to the gas adsorption experiments and also imply the efficient inclusion of a larger guest in a dynamic fashion of **1**. Other guest molecules larger than toluene, such as *o*-methoxyphenol ($\text{C}_7\text{H}_8\text{O}_2$) and 1-chloronaphthalene ($\text{C}_{10}\text{H}_7\text{Cl}$), were also tested. As *o*-methoxyphenol and 1-chloronaphthalene are glutinous, TG analyses of the mass steps of $1 \cdot x'\text{C}_7\text{H}_8\text{O}_2$ and $1 \cdot y'\text{C}_{10}\text{H}_7\text{Cl}$ are difficult to test. However, no obvious displacement and change appear in the XRPD patterns, implying no inclusion of these two species because of the more obvious steric hindrance and larger molecular size than

those of benzene and toluene. This fact further indicates that the size and shape of larger guest and the “dynamic” window must be matched during the solid–liquid crystalline-state guest inclusion under normal temperature.^{7,19}

Conclusions

This work shows that a linear 1D coordination polymer may be packed efficiently into a porous framework solid with large interlinked voids hosting solvent molecules. The resulting framework of **1** is robust and can remain intact after guest removal or readsorption. The guest-exchange studies show that small molecules MeOH and *i*-PrOH may be incorporated into the lattice voids without alteration of the host framework structure. Gas sorption and guest inclusion in benzene and toluene solutions confirmed that the material is porous and can uptake/fetter benzene and toluene, albeit the size of the guests is slightly larger than the windows of the host channels. This compound may also serve a candidate for dynamic porous material. Finally, our results provide a hint for the design of a “soft” supramolecular framework with low dimensional building blocks consolidated by supramolecular interactions.

Acknowledgment. This work was supported by NSFC (No. 20561001), the Program for New Century Excellent Talents in University of the Ministry of Education China (NCET-07-217), GKN (Grant 0630006-5D), as well as the Scientific Foundation of GuangXi Province (No. 0731053).

Supporting Information Available: Figures of TG curves and IR spectra for $1 \cdot \text{H}_2\text{O}$, $1 \cdot \text{MeOH}$, and $1 \cdot i\text{-PrOH}$ (PDF). This material is available free of charge via the Internet at <http://pubs.acs.org>.

IC800050U